

TRAINING ULTRA LONG CONTEXT LANGUAGE MODEL WITH FULLY PIPELINED DISTRIBUTED TRANSFORMER

Jinghan Yao^{* 1} Sam Ade Jacobs² Masahiro Tanaka² Olatunji Ruwase² Aamir Shafi¹ Hari Subramoni¹
Dhableswar K. (DK) Panda¹

ABSTRACT

Large Language Models (LLMs) with long context capabilities are integral to complex tasks in natural language processing and computational biology, such as text generation and protein sequence analysis. However, training LLMs directly on extremely long contexts demands considerable GPU resources and increased memory, leading to higher costs and greater complexity. Alternative approaches that introduce long context capabilities via downstream finetuning or adaptations impose significant design limitations. In this paper, we propose Fully Pipelined Distributed Transformer (FPDT) for efficiently training long-context LLMs with extreme hardware efficiency. For GPT and Llama models, we achieve a 16x increase in sequence length that can be trained on the same hardware compared to current state-of-the-art solutions. With our dedicated sequence chunk pipeline design, we can now train 8B LLM with 2 million sequence length on only 4 GPUs, while also maintaining over 55% of MFU. Our proposed FPDT is agnostic to existing training techniques and is proven to work efficiently across different LLM models. The code is available [here](#).

1 INTRODUCTION

The rapid advancement of large language models (LLMs) has significantly impacted natural language processing (NLP), driving improvements across a wide range of applications. As LLMs like GPT-4, Claude, and Gemini become increasingly capable of processing regular prompts, there is a growing demand to extend their context windows to accommodate longer input sequences. This capability is crucial for a variety of applications, including comprehensive document analysis, where models must process entire legal documents or scientific papers (Peng et al., 2023; Xiong et al., 2023); long-form content generation, such as writing books or detailed reports; maintaining coherent and contextually relevant long-term dialogues in conversational AI (Beltagy et al., 2020; MosaicML, 2023; Munkhdalai et al., 2024; Touvron et al., 2023); and handling complex multi-step reasoning tasks in fields like healthcare (Gao et al., 2021; Li et al., 2022; Zvyagin et al., 2023), climate (Nguyen et al., 2023), and finance (Eisfeldt et al., 2023; Kim et al., 2023; 2024; Li et al., 2023; Yang et al., 2023).

However, LLM training is typically constrained to relatively short context lengths, such as 8K or 32K tokens. Currently,

^{*}Work done while intern at Microsoft. ¹The Ohio State University ²Microsoft Inc. Correspondence to: Jinghan Yao <yao.877@osu.edu>, Sam Ade Jacobs <samjacobs@microsoft.com>.

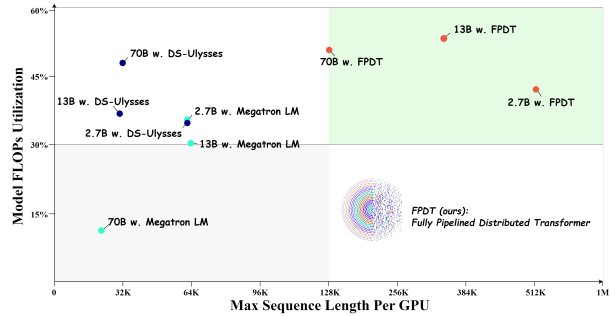


Figure 1. Comparison of end-to-end training Model FLOPs Utilization (MFU) and maximum context length per GPU supported. We show 3 model sizes, i.e. 2.7B, 13B, and 70B.

most LLMs utilize rotary position embedding (Su et al., 2024) (RoPE) to encode input tokens. Despite its improved efficiency and extrapolation capability compared to regular position embeddings (Vaswani, 2017), to accommodate much longer prompts during inference, RoPE often requires aggressive rescale and map. These adjustments struggle in properly adapt models to longer context before the model’s performance deteriorates, leading to a collapse in the quality of its outputs. This presents a critical challenge: the necessity to train LLMs originally on the desired long context lengths to ensure robust performance across varying applications.

There are multiple difficulties in training long-context LLMs. For a given-sized LLM model, as we increase the sequence

Model size	Hardware configuration							
	A100 40G				A100 80G			
	1	2	4	8	4	8	16	32
2.7B	128K	512K	2M	4M	4M	8M+	8M+	8M+
8B	-	-	-	1M	2M	4M	8M+	8M+
13B	-	-	-	256K	512K	3M	4M	8M+
30B	-	-	-	-	-	1M	3M	4M
70B	-	-	-	-	-	-	1M	4M

Table 1. Maximum context length supported for LLM training with our FPDT design. + denotes we only test to this length. - denotes that the model itself cannot fit into GPU memory.

length during training, the memory needed for storing activations and intermediate buffers increases proportionally, while the model parameters and optimizer states remain at a certain point. As we identified in this paper, this increase in activation memory can lead to severe GPU memory pressure. Previous memory-efficient techniques, such as FlashAttention (Dao, 2023; Dao et al., 2022), have been proposed to alleviate the memory burden of materializing the giant QK^T matrix, reducing memory complexity from $O(N^2)$ to $O(N)$, though, it still has a non-trivial constant factor which can easily cause out-of-memory issues when the sequence length grows to millions of tokens. Methods like Megatron-SP (Korthikanti et al., 2023) and DeepSpeed Ulysses (Jacobs et al., 2023) have been proposed to leverage distributed GPU clusters. Megatron-SP adopts tensor parallelism to distribute the computation and memory of long sequences. In contrast, DeepSpeed Ulysses leverages the multi-head attention feature in current LLM models, using efficient all-to-all communication to distribute context head-wise, thereby easing memory pressure.

These sequence parallel strategies, despite being proven the feasibility of training LLMs with long contexts, require a substantial number of GPUs. For instance, training a 7B parameter model with a context window of 256K tokens using Megatron-SP results requires more than 32 A100 80G GPUs. Similarly, training a small 1.2B parameter GPT model with a 1M token context length using DeepSpeed Ulysses requires 64 A100 GPUs. These costly hardware pose severe usability challenges for companies and individual researchers with limited resources. Although with existing techniques such as activation checkpoint, the above solutions can extend further to longer sequence length, we identify that none of them can meet the expectation.

In this work, we aim to address these challenges by proposing a new **Fully Pipelined Distributed Transformer (FPDT)** for training long-context LLMs. Our method leverages the multiple memory hierarchies in modern GPU clusters, enhancing their hardware efficiency and cost-effectiveness while reaching extremely high MFU.

Our contributions are as follows:

- We provide an end-to-end analysis of the memory footprint of LLM training, identifying memory spikes concerning commonly used Transformer architectures, and targeting on reducing redundant intermediate buffers in forward and backward passes respectively.
- We design a fully pipelined distributed transformer based on DeepSpeed Ulysses, tailored for **LLMs with sequence lengths of millions of tokens**, leveraging both GPU and host CPU memory as well as prefetching, to achieve a near-zero overhead training flow.
- We significantly reduce the GPU memory footprint of activations during the training of LLM, while leveraging a dedicated double buffer design to overlap almost all prefetching with computation.
- As shown in Table 1, our proposed method supports training 8B LLMs on over 2M sequence with only 4 GPUs, or 70B models on 4M sequence with 32 GPUs, which can be up to 16x longer than existing solutions, while reaching over 55% of MFU.
- Our solution works orthogonally and composably with DeepSpeed ZeRO family (Rajbhandari et al., 2020) and PyTorch FSDP (Zhao et al., 2023) of memory optimizations, and can be applied to Transformer-based models of any size, such as GPT, Llama, etc.

2 RELATED WORK

2.1 Memory-efficient Transformer

The substantial memory demands of Transformers have spurred extensive research into memory-efficient attention mechanisms to facilitate their application to longer sequences. FlashAttention (Dao, 2023; Dao et al., 2022) has emerged as the de facto standard due to its robust and versatile performance. FlashAttention employs an online softmax technique to avoid the materialization of the attention matrix, thereby reducing memory overhead from $O(N^2)$ to $O(N)$ while preserving accuracy. Other notable strategies include low-rank approximations (Katharopoulos et al., 2020; Wang et al., 2020), kernel-based methods (Kitaev et al., 2020;

Lu et al., 2021; Xiong et al., 2021), and sparse attention mechanisms (Child et al., 2019), which approximate or selectively compute attention to minimize memory consumption. Furthermore, techniques that combine local and global contexts (Ainslie et al., 2020; Beltagy et al., 2020; Liu et al., 2021; Zaheer et al., 2020) enable superior performance on tasks involving long sequences or large-scale inputs while maintaining computational efficiency. Our work is inspired by FlashAttention and builds upon it by introducing hierarchical blockwise computation, leveraging the memory hierarchy in modern systems, which significantly enhances scalability and reduces memory requirements.

2.2 Long context training

Recent advancements in Transformer architectures have significantly enhanced their capability to process long sequences, which is crucial for tasks that require extensive contextual understanding. This section reviews pivotal contributions in this domain, each addressing the inherent memory limitations of standard Transformer models, while also pointing out some of their practical challenges.

Megatron-SP (Korthikanti et al., 2023) adopts a sequence parallelism technique which is tightly integrated with its tensor parallelism. In this approach, sequences are partitioned along the sequence dimension, and all-gather and reduce-scatter collectives are employed to aggregate the QKV (query, key, value) projections for attention computation. The communication complexity analysis indicates that, in contrast to our approach, the communication volume in Megatron-SP’s sequence parallelism increases linearly with the message size (M) regardless of the number of compute devices.

The Blockwise Parallel Transformer (BPT) (Liu & Abbeel, 2024) employs a blockwise computation strategy for both self-attention and feedforward layers, optimizing memory usage and allowing the processing of sequences much longer than traditional Transformers. However, despite its efficiency, BPT requires careful tuning of block sizes and memory management to avoid diminishing returns on performance when scaling to extremely long sequences.

Ring Attention (Liu et al., 2023) enhances Transformer’s scalability by distributing long sequences across multiple devices. This innovative approach overlaps the communication of key-value pairs with the computation of blockwise attention, effectively increasing the feasible sequence length proportionally to the number of available devices. However, reliance on device count for scaling and multi-step communications introduces potential issues in environments with sub-optimal hardware, where performance can be unpredictably affected by network latency and bandwidth constraints.

DeepSpeed Ulysses (Jacobs et al., 2023) tackles the challenges of sequence parallelism by partitioning input data along the sequence dimension and utilizing an efficient all-to-all collective communication strategy for attention computations. Although this method maintains a constant communication volume regardless of the increase in sequence lengths and device counts, achieving significant speedups and scalability, it may still encounter practical hurdles in deployment related to large-scale clusters and the optimization of collective communication patterns across diverse computing environments.

Each of these methods uniquely contributes to the field of long-sequence Transformer training, offering solutions focused on memory efficiency, communication overhead, and computational speed. However, the common requirement for substantial GPU resources in all these approaches underscores a critical barrier to broader adoption and scalability. This challenge highlights the need for future research to develop more resource-efficient methods that can deliver similar benefits with a modest hardware budget.

Besides above mentioned large-scale training techniques, several recent works focus on long-sequence LLM training on small-scale GPU clusters. MsT (Luo et al., 2024) adopts a chunking mechanism on MLP and loss computation, which showed benefits in reducing GPU memory consumption. However, as we will mention later, attention computation can incur the most significant memory spikes during training, which remains unsolved in their method. MEMO (Zhao et al., 2024), on the other hand, targets reducing memory in the attention part by using host memory for offloading. Their method requires integer programming solvers, and since it is built up on the tensor parallel scheme, failing to achieve optimal hardware efficiency in long-sequence training scenarios.

3 PRELIMINARY

3.1 GPU memory requirements in distributed Transformer

Table 2. Memory footprint at each step in a Transformer block

	Hidden	QKV proj.	All2all	Attention	FFN	Other ops.
	Activations					
Forward	Nd	$3Nd$	$4Nd$	$4Nd$	$4Nd$	$3Nd$
Backward	$2Nd$	$6Nd$		$8Nd$	$8Nd$	

As Transformer becomes the de facto most powerful and ubiquitous architecture in today’s generative models, its overall pipeline also becomes homogeneous. We use the

following table to show the required GPU memory at each step in forward and backward of a Transformer block.

Noticeable in this table, is that to get query, key, and value, the memory footprint is directly increased by three times, which solely can potentially lead to an out-of-memory issue when the sequence itself is too long to fit in the GPU memory. Also, as most Alltoall implementations do not support in-place operation, we need to create a receive buffer in addition to the input buffer. And if asynchronous communication is enabled, we need to prepare the receive buffer for query, key, and value at one time, leading to an $6Nd$ memory footprint.

FlashAttention is introduced to reduce the memory consumption to $O(N)$, however, in practice, it can also incur a huge memory footprint. For example, in backward, FlashAttention requires the following inputs: $q, k, v, o_f, o_g, dq, dk, dv$, where o_f denotes the attention output of the forward pass, and o_g denotes the gradient of output in the backward pass. As these tensors need to be present in GPU memory at one time, it directly leads to a $8Nd$ memory footprint. We identify that none of the existing solutions exclusively target these memory burdens, which, however, becomes salient in long-context LLM training.

3.2 Combining DeepSpeed sequence parallel and ZeRO

Among sequence parallel strategies, DeepSpeed-Ulysses excels with its highly efficient communication pattern and is complementary to the most advanced model-based training schemes such as DeepSpeed ZeRO. We first recap the key feature of DeepSpeed Ulysses, and how it can work with ZeRO-3.

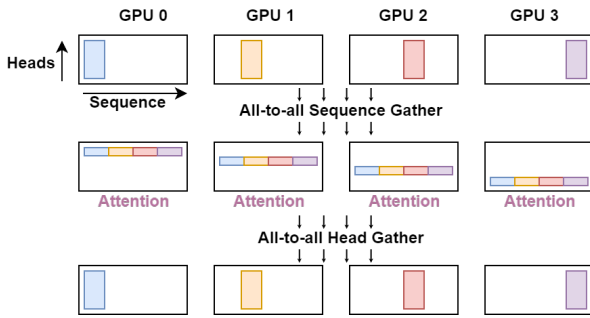


Figure 2. DeepSpeed Ulysses with distributed attention.

Figure 2 (a) shows the communication pattern of DeepSpeed Ulysses sequence parallelism. Each GPU initially has a piece of the entire sequence with full heads, when performing attention, sequence pieces are gathered to each GPU, while heads are scattered to different GPUs. ZeRO3 partitions all parameters, gradients, and optimizer states along a data-parallel GPU group. As sequences consist of

tokens, they can be easily treated as batches of data, where we can directly apply the data parallelism. As shown in Fig 3, in this combined training scheme, sequence parallel is used to reduce activation memory, and ZeRO-3 reduces the model-related memory.

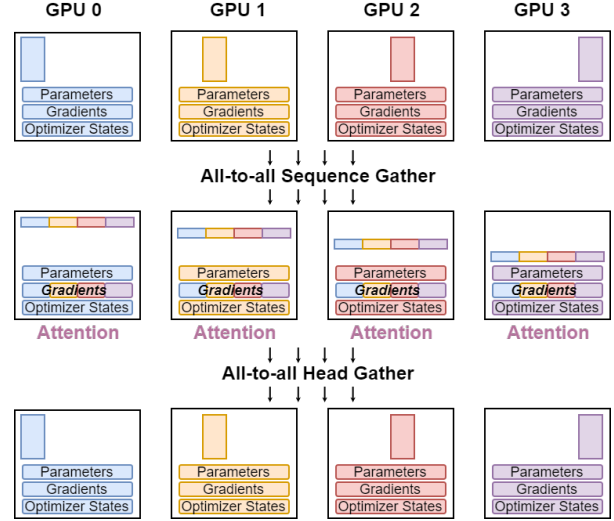


Figure 3. DeepSpeed Ulysses works orthogonally with ZeRO-3.

4 DESIGN OF FULLY PIPELINED DISTRIBUTED TRANSFORMER

In this section, we start by introducing how to design a seamless and efficient pipelined distributed attention with offloading. Since different hardware hierarchies are involved in the design, e.g. Tensor cores, NVLINK, PCIe, etc, each with different data throughput and latency, they are required to coordinate carefully.

4.1 Pipelining and scheduling

As QKV projection, Alltoall communication, attention, and FFN will create multiple intermediate buffers, leading to severe memory spikes, especially during the backward pass, to make the sequence computation in the Transformer block fully pipelined and memory efficient, our chunk and offloading design will start with the initial input tensor (i.e. hidden state). Firstly, we use the following notations throughout the paper for ease of explanation. For operations other than the distributed attention, each GPU holds and processes a $[b, s_{local}, h_{global}, d]$ tensor, where s_{local} denotes the local sequence length, h_{global} denotes the total number of heads. For the distributed attention, each GPU will process the entire sequence, but with specific heads, which is a $[b, s_{global}, h_{local}, d]$ tensor.

For the first QKV projection, since tokens are processed elementwise, we directly slice the local sequence tensor $[b, s_{local}, h_{global}, d]$ into u chunks, each as a

$[b, \frac{s_{local}}{u}, h_{global}, d]$ tensor. We denote these chunks as T_i , where $i \in \{0, 1, \dots, u-1\}$. As shown in Figure 4, c_i is projected to query q_i , key k_i , and value v_i . Then, we perform the Alltoall communication among the sequence parallel group. Recall that in table 2, we mentioned that since Alltoall communication cannot be performed in-place, additional receive buffers need to be pre-allocated. In our chunk design, as we largely reduced the sequence length by a factor of u , even though the receiving buffers for $\hat{q}_i, \hat{k}_i, \hat{v}_i$ are still required, they become trivial compared to the original sequence tensor with full context.

Distributed Attention with Offloading

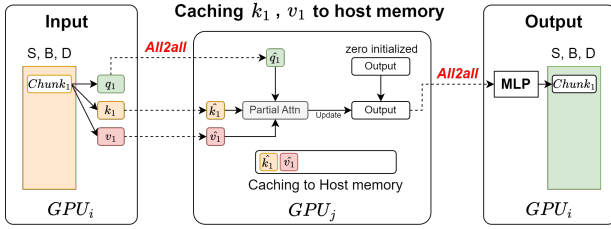


Figure 4. The design of distributed attention with offloading

After using Alltoall to scatter heads and gather sequence, each chunk $\hat{q}_i, \hat{k}_i, \hat{v}_i$ is a $[b, \frac{s_{global}}{u}, h_{local}, d]$ tensor. Note that, for generative LLMs, due to the casual mask, after the computation, \hat{q}_i will not be used in the forward pass anymore, while \hat{k}_i, \hat{v}_i need to participate in the following \hat{q}_j computation, where $i < j$. Therefore, we cache \hat{k}_i, \hat{v}_i to the host memory. Specifically, for $\hat{q}_0, \hat{k}_0, \hat{v}_0$, we can directly get the final output of chunk T_0 , as \hat{q}_0 will not attend to the remaining sequence. For chunk $T_i, i \geq 0$, processing each chunk only gives intermediate results, which will be rescaled in the next chunk computation. As online attention is widely used, we adopt a similar strategy when scheduling the attention computation.

Distributed Attention with Fetching/Offloading

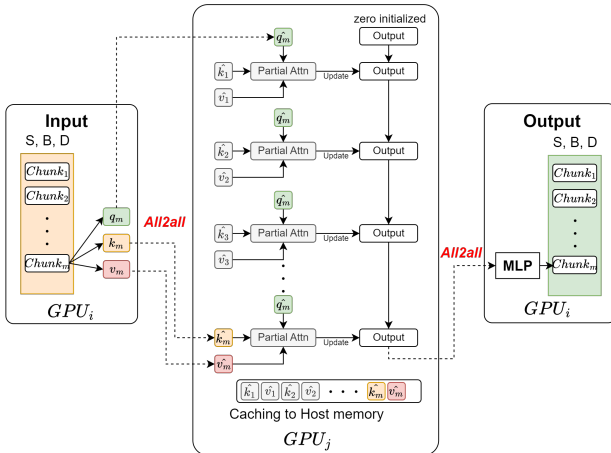
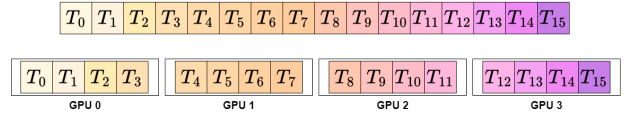


Figure 5. The design of distributed attention with fetching and offloading. We follow the online attention policy to update attention output.

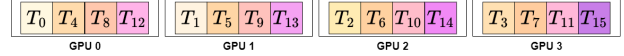
Figure 5 gives an example of how to perform the computation of chunk T_m . After the Alltoall operation, GPU_j receives \hat{q}_m, \hat{k}_m , and \hat{v}_m . We then fetch the previous sequence chunk by chunk from the host memory to GPU_j , and perform online attention with the current \hat{q}_m , and update the output chunk accordingly. Note that, in a strict manner, at any given time, only one set of chunks \hat{k}_i, \hat{v}_i is placed on GPU's HBM, reducing the memory footprint to $\frac{1}{u}$ compared to the non-offloading version.

Unlike inference, where activations and intermediate results can be freed as soon as the forward pass of the current Transformer block finishes, training requires saving necessary intermediate outputs as it is reused in the backward pass. Therefore, we offload $\hat{q}_i, \hat{k}_i, \hat{v}_i$ to the host memory once they are done for forward computation.

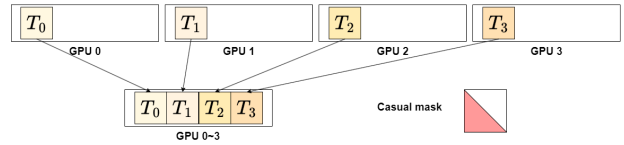
Placement of sequence w/o. pipelining



Placement of sequence w. pipelining



1st Alltoall sequence gathering (head scattering):



4th Alltoall sequence gathering (head scattering):

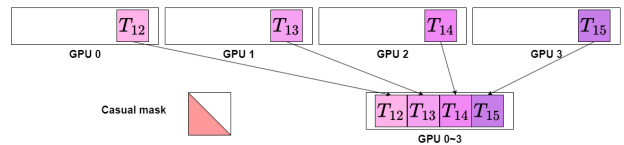


Figure 6. Rank ordinal scattering of sequence chunks. The diagonal casual mask remains valid after each chunk Alltoall operation. NVLINK is also load-balanced in this data layout.

Before diving into more advanced designs, we need to shuffle the sequence accordingly due to the chunked Alltoall sequence gathering. In the original sequence parallel scheme, the input sequence is sliced and dispatched to each GPU based on their rank. As shown in Figure 6, if we directly perform the Alltoall operation on the i_{th} chunk on each GPU, then the sequence we gather does not conform to the casual mask.

For example, when gathering the second chunk, each GPU will get a sequence consisting of chunk T_1, T_5, T_9, T_{13} with rank-specific heads. However, since each GPU has already received T_0, T_4, T_8, T_{12} in the previous chunk computation,

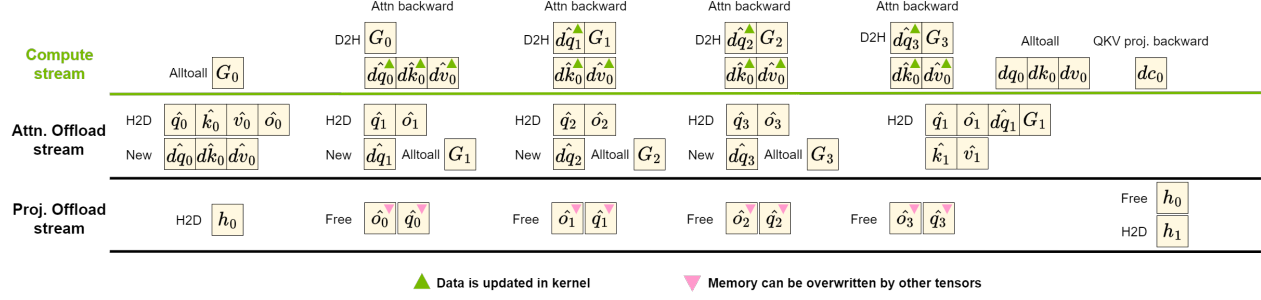


Figure 7. Double buffer leverages multiple CUDA streams in the backward pass of a Transformer block. We overlap most offloading operations with the attention gradients computation.

the casual mask for \hat{q}_1, \hat{k}_0 needs to be dedicatedly designed, as T_5 can only attend to tokens in T_0 and T_4 , etc. Another workaround would be to only let i_{th} GPU scatter its sequence to all GPUs, this does not require reordering the sequence, but will result in NVLINK load imbalance. During training, since each GPU computes the loss of the sequence it holds, we also reorder the labels accordingly, so that the loss still matches. Note that we shuffle the input token ids and labels in the data loader; thus, there is no overhead in this reordering of sequence.

We also emphasize that, unlike Ring Attention, in our design, each GPU always processes the same piece of sequence at any given time, with the only difference in rank-specific heads. Therefore, GPUs are always load-balanced when computing attention. This uniform workflow also reduces the synchronization and barrier required to coordinate the sequence of the parallel group.

4.2 Double buffering

Though the idea of using host memory to hold unused sequences is intuitive, the unmatched hardware transfer bandwidth poses a significant challenge in fully exploiting computing power. For a typical HPC node, GPUs are connected through high-bandwidth NVLink, which can reach more than 100 GB/s of peer-to-peer bandwidth. However, the common PCIe Gen-4 link with 16 lanes only provides 32 GB/s of unidirectional bandwidth, which also requires the host memory and GPU to be in the same NUMA domain.

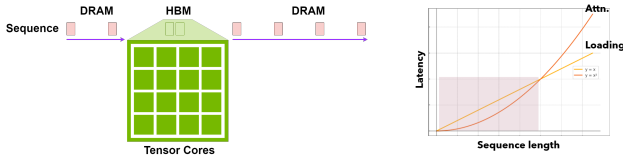


Figure 8. Short sequence chunk leads to GPU starving.

Figure 8 shows a GPU starving case where the sequence

chunk is too short such that the latency in the attention computation is less than the data fetch latency. In this situation, the training will be bound by the PCIe bandwidth, leading to low Model FLOPs Utilization (MFU).

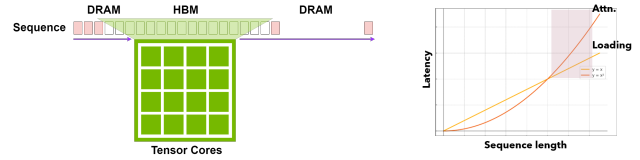


Figure 9. Long sequence chunk leads to HBM wasting.

Figure 9 shows an opposite case where each sequence chunk is too long. Because the tensor we passed to a kernel (i.e. attention forward/backward kernels) needs to reside on HBM as a whole, it will take too much GPU memory, which becomes unnecessary, as tokens can be fetched from host memory as soon as previous ones are computed.

Furthermore, the mismatch in GPU computing throughput and PCIe link bandwidth also poses a severe difficulty in efficiently incorporating offloading into the regular computation pipeline. Figure 10 shows the latency of different operations performed on our GPU node (see 5.1 for details). Note that here we compare the actual tensor operations in a transformer block, i.e. Alltoall on $[b, \frac{s}{p}, h, d]$ tensor, attention on $[b, s, \frac{h}{p}, d]$ tensor, and fetching on $[3, b, s, \frac{h}{p}, d]$ tensor which represents the query, key, and value. As the complexity of attention computation increases quadratically, it easily dominates the overall latency if we let each sequence chunk be large enough (e.g. 512k), in which case the latency of communication and fetching becomes negligible. In practice, however, a large chunk size also increases the memory pressure, which is against our initial goal. Finding the sweet point between fully utilizing computing cores and hiding the latency of offloading/fetching is crucial for achieving the optimal training efficiency. As shown in Figure 10, Alltoall is much faster since this is only

the intra-node communication using NVLink.

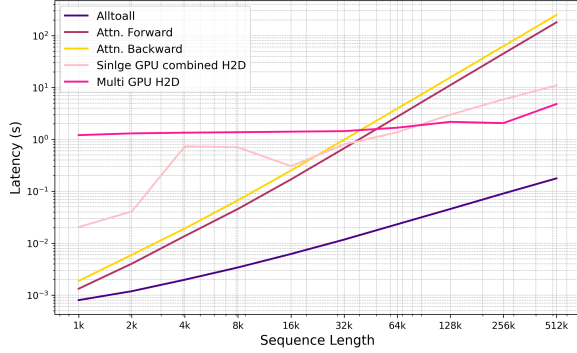


Figure 10. Average Time Spent in Alltoall, Attention Forward, Attention Backward, and three different host-to-device fetching strategies.

Thus, we care more about when the latency of attention computation overpasses that of host-to-device fetching. Unlike inter-GPU connections, data transfer among host memory and GPUs is not homogeneous. In our case, all GPUs will share the PCIe bandwidth, especially when host-to-device memory copy is issued simultaneously on each GPU. Therefore, we investigated two different strategies for fetching data from host memory to the corresponding GPUs. The most intuitive way is to let each GPU issue its own *HtoD* transferring, which can make use of all DMA engines available, however, this might lead to resource contention as each GPU will try to consume some PCIe bandwidth as well as PCIe lanes. The second strategy is to let one GPU in each node fetch all related tensors, and then use a scatter operation to send corresponding chunks to other devices. In our profiling, we found that though the multi-GPU *HtoD* strategy performs worse at smaller data sizes, due to the overhead in lane contention, latencies of both methods are overpassed by attention computation at around 32k to 64k, and thus, their difference becomes negligible as the sequence length grows larger. Since fetching from one GPU and scattering to other GPUs require additional synchronization and barrier, we choose the first strategy where we allow every GPU to fetch its data without any additional synchronization.

Figure 7 illustrates our double buffer workflow. Note that here we show the backward pass of our FPDT block, as the forward workflow is simpler and can also be reflected by examining the backward pass. We assume that there are 4 chunks in total. Since the global sequence chunk $\hat{q}_i, \hat{k}_i, \hat{v}_i$ have been cached during the forward, we then directly fetch them from the host memory without introducing additional Alltoall. We use a nested loop to compute and update the gradients of query \hat{dq}_i , key \hat{dk}_i , and value \hat{dv}_i . The outer loop is on key and value, while the inner one is on query.

This design ensures that the attention computation in the inner loop only needs to cover the latency of fetching the next query, otherwise, it will need to cover both key and value prefetching. In the inner loop, since \hat{k}_0 and \hat{v}_0 are used by $\hat{q}_0, \hat{q}_1, \hat{q}_2, \hat{q}_3$, we therefore update \hat{dk}_0, \hat{dv}_0 each time. For \hat{dq}_0 , we get its final result after the first inner loop, which is due to the autoregressive nature of LLM that q_i never attends to k_j if $i < j$. Similarly, we get the final results of \hat{dk}_0 and \hat{dv}_0 after the first outer loop. Then, we initiate Alltoall to scatter the global sequence chunk to its original GPU, where dq_0, dk_0, dv_0 are used to compute the gradient of the input hidden state dc_0 . Note that here we also overlap Alltoall and projection backward with the prefetching of \hat{q}_1, \hat{k}_1 , and \hat{v}_1 , which will be used in the next outer loop. In our implementation, we deploy three CUDA streams, as the prefetching of the input hidden state h_0 will only be synced in the projection backward. For chunk buffers that will never be used after each inner loop, we mark them as free memory, which can be allocated to the following chunks.

5 EVALUATION

5.1 Experimental Setup

Models: We conduct our main experiments using the GPT and Llama models, with model sizes ranging from 2.7B to 70B. By default, we enable activation checkpoint with CPU offloading. To fully exploit the potential of FPDT, we use DeepSpeed ZeRO-3 to partition the model parameters across the sequence parallel group (refer to 3.2). We also set the batch size to 1, as this allows us to test the maximum sequence length we can reach.

Experimental Environment: We use multiple GPU nodes, each with four A100 80 GB, connected via 3rd-Gen NVLink. There are two CPU sockets. The PCIe between host and device has a theoretical uni-directional bandwidth of 32 GB/s. Each node is equipped with 1 TB of host memory. For the internode connection, we use NVIDIA 200 Gbps HDR InfiniBand.

5.2 Overall Performance

There are several widely used solutions for training long-context language models. Megatron-SP (Korthikanti et al., 2023) partitions sequence activations and leverages tensor parallel. DeepSpeed Ulysses (Jacobs et al., 2023) adopts a one-step Alltoall to gather tokens and scatter heads among all GPUs. In this section, We compare our proposed design with these state-of-the-art solutions.

We choose six widely used LLM models with different sizes. For GPT-like ones, we have 2.7B, 6.7B, 13B, and 30B. For Llama, we use the 8B and 70B models. For Megatron-SP, we follow its default parallel setting, which leverages tensor

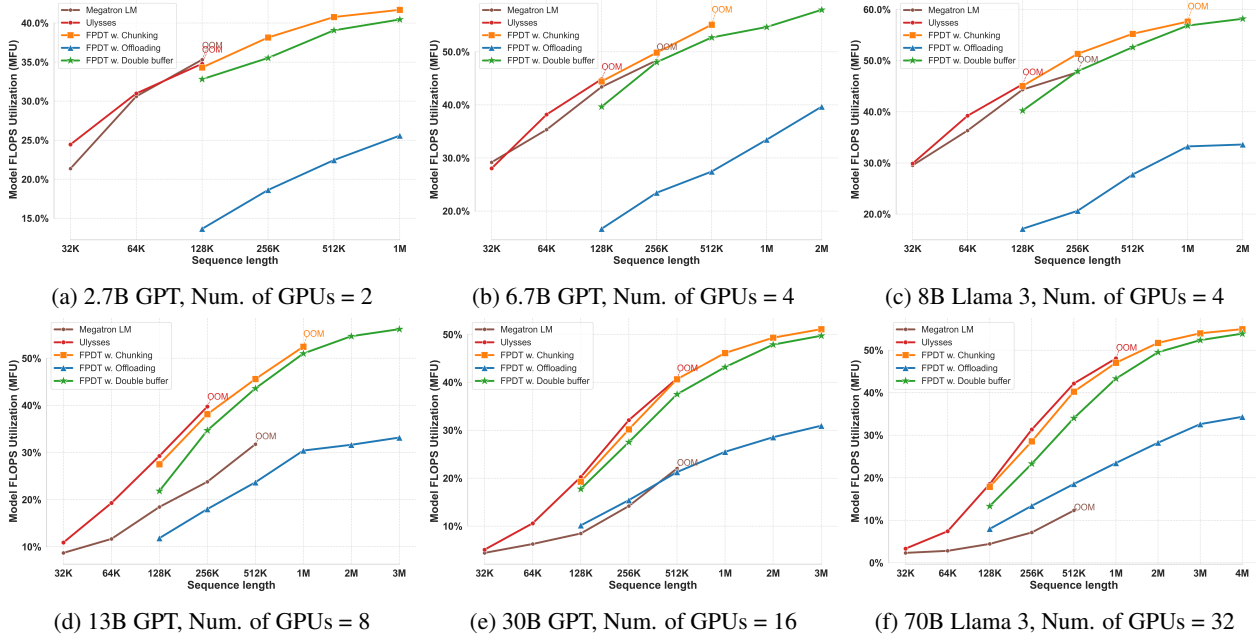


Figure 11. Supported sequence lengths and corresponding Model FLOPs Utilization (MFU) using Megatron-SP, Ulysses, and our proposed FPDT. OOM denotes the point where increasing sequence length will cause memory issues. We show FPDT’s performance when the sequence length is larger than 128K, as shorter sequences can be properly handled by existing strategies.

model parallel and sequence parallel. For our proposed FPDT, ZeRO-3 model parameter sharding is leveraged, this ensures fair comparison between Megatron-SP, DeepSpeed Ulysses, and FPDT. For all experiments, we set the batch size to 1 and enable the activation checkpoint with CPU offloading. Our goal is to fully exploit the long sequence handling capability of each parallel strategy.

Table 11 shows the end-to-end training performance. When running within one compute node, Megatron-SP and Ulysses exhibit similar hardware efficiency. For example, on the 2.7B GPT model, both methods have a maximum sequence length of 256K. For our proposed FPDT, with only chunking, we increase the sequence length by 8x longer, from 256K to 2M, without sacrificing performance. For the 6.7B GPT model, Megatron-SP and Ulysses support 128K and 256K sequence lengths. Our FPDT with chunking increases the bound to 512K while facing out-of-memory (OOM) issues when we keep increasing the sequence length. We then leverage the host memory. By offloading idle tokens from HBM, we support the 2M sequence length, which is 8x longer than the existing solutions. By properly managing the offloading, fetching, and computation, our FPDT with double buffer strategy reaches comparable hardware MFU as the non-offloading counterparts (i.e. FPDT w. chunking). Similar results are also shown in the 8B Llama 3 model training. As we increase the model’s size, we scale it up to multiple nodes. We found that Ulysses is generally more efficient than Megatron-SP, as the latter’s performance de-

grades severely when inter-node communication is included. For the 13B, 30B, and 70B models, we use 2, 4, and 8 nodes, respectively. While both Megatron-SP and Ulysses struggle with the memory spikes of activations, our FPDT works effectively by increasing the maximum sequence length to 2M while maintaining high MFU.

5.3 Tradeoff on Sequence Chunk Size

As discussed in 4.2, choosing a proper chunk size can not only exploit the computing power of the hardware but also allow the data moving from host to device and from device to host to overlap by computation. In Table 11, we use a default chunk size of 64K for all our FPDT-based methods. In this part, we will demonstrate why this is our preference. Table 12 shows the usage of GPU HBM at different chunk lengths. We conduct the profiling on a single node with 4 GPUs, with a fixed global sequence length of 256K. We change the length of each sequence chunk and compare the corresponding memory footprint and MFU. The chunk size of 256K means that we do not use chunk, but just run the baseline Ulysses. 8K, 16K, 32K, 64K, and 128K of chunk size corresponds to 32, 16, 8, 4, and 2 chunks in total in our FPDT pipeline scheme. As shown in Figure 12a, 12b, 12d, our FPDT can significantly reduce the activation memory footprint; for example, in the 2.7B model, we reduce the activation memory from 27GB to 18GB by splitting the sequence into two chunks. Despite that increasing the number of chunks can further reduce the memory footprint, we

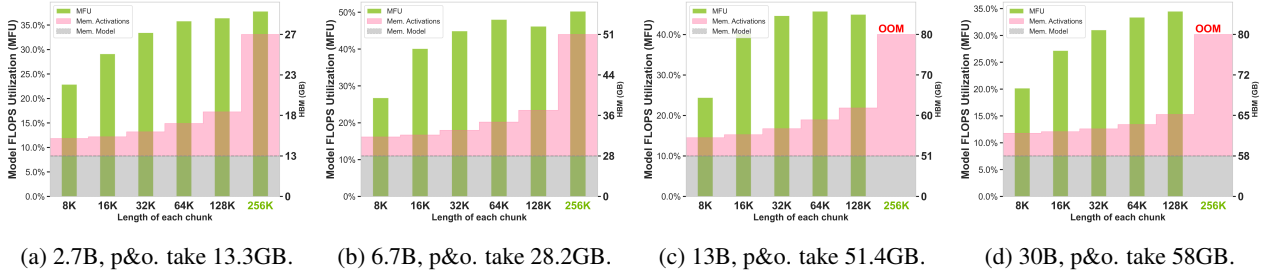


Figure 12. MFU and HBM memory consumed during training. The global sequence length is set to 256K, and we change the chunk size. We use 4 GPUs for 2.7B, 6.7B, and 13B models; 8 GPUs for 30B model. Gray areas represent the memory taken by model parameters and optimizer states (**p&o.**). Pink areas represent the memory taken by activations.

found that 64K is a sweet point where the latency of offloading and prefetching can be hidden by the computation. Less chunks means a shorter pipeline, which makes latencies of the first data preparation and the last computation more salient, as they cannot overlap with other operations. More chunks, however, make the latency of computation too short to hide that of data loading. Therefore, we choose 64K as it has an overall best-overlapped pipeline.

5.4 Chunk Granularity

As we analyzed in table 2, in forward and backward passes, attention operation and FFN can incur different amounts of intermediate buffers, therefore, different chunking strategies need to be applied. The chunking and offloading strategies of the attention part have been introduced in 4.2. For FFN, however, we cannot easily leverage offloading to reduce GPU memory consumption without significantly sacrificing hardware efficiency. For token-wise operations such as FFN, the complexity of computation increases linearly, i.e. $O(N)$. In this case, $F(N) = \Theta(G(N))$, where F and G are the complexities of compute and memory, respectively. Considering the high throughput of GPU compute cores, the latency of offloading and prefetching can never be overlapped by computation, thus, for FFN, we don’t use offloading. Figure 13 are the memory profiles created by the PyTorch profiler (note that PyTorch randomly picks colors in each profile), we found that for the GPT and Llama models, setting the number of chunks in the FFN to be twice that of the attention is sufficient to ensure that the attention part strictly binds the memory footprint.

Also noteworthy is that since we do not offload chunks in FFN, as long as the size of each chunk is not too small, the overall training throughput would not be significantly affected. We also want to emphasize that another memory spike during training is found in the final calculation of softmax and cross-entropy loss. As the vocabulary size is much larger than the model’s hidden dimension, and the operation usually requires a `Float32` data type, the last linear project would lead to the out-of-memory issue.

However, this part can be solved by chunking as well, and since it is at the end of the forward pass, the number of chunks used in this part is trivial to the overall performance. Thus, we suggest that setting it to $\frac{vocab_size}{hidden_dim} \times 2$, would solve the memory spike.

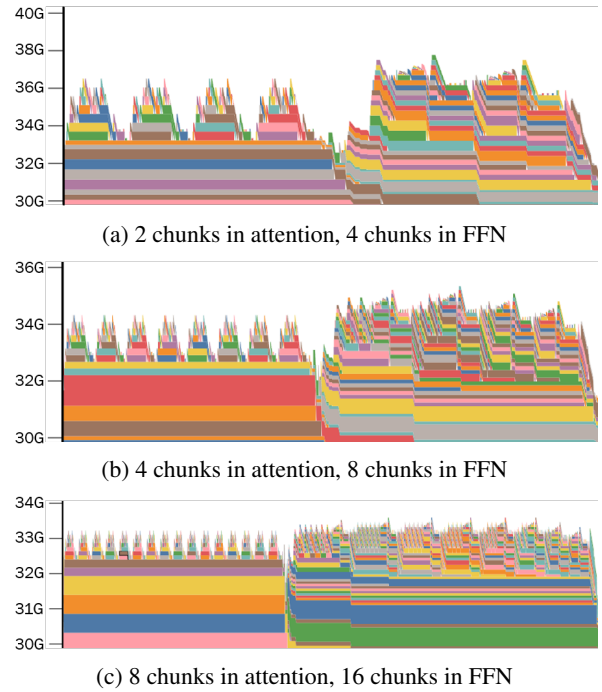


Figure 13. Memory footprint in the backward pass of a Transformer block in Llama 8B. We first calculate the gradients in FFN, then the attention. FFN uses 2x chunks of attention.

5.5 Training strategies in long-context LLM

Though we discussed our experiments’ setup in 5.2, we would like to know how each strategy contributes to the long-context LLM training. Tensor parallel is widely used in distributed model training. It allows each GPU to only keep a slice of the tensor along the hidden dimension, hence

	Training strategies								Performance		
	TP.	AC.	OC.	UL.	ZeRO-1	ZeRO-2	ZeRO-3	FPDT	Max len.	HBM.	MFU
8B Llama 3 8 GPUs	✓								32K	64.3G	9.4%
	✓	✓							128K	61.2G	19.4%
	✓	✓	✓						512K	78.7G	32.7%
				✓	✓				64K	58.9G	15.3%
				✓		✓			64K	54.5G	15.3%
				✓			✓		64K	52.3G	21.0%
		✓	✓	✓	✓				512K	65.5G	46.8%
		✓	✓	✓		✓			512K	65.5G	46.8%
		✓	✓	✓			✓		512K	60.1G	47.2%
		✓	✓				✓	★	4M	68.0G	55.7%

Table 3. A comprehensive analysis on long-context LLM training with different training techniques. **TP.** denotes tensor parallel. **AC.** denotes activation checkpoint. **OC.** denotes activation checkpoint with CPU offloading. **UL.** stands for Ulysses. **FPDT** is our proposed Fully Pipelined Distributed Transformer.

also parallelizing the computation. However, it cannot reduce the memory footprint of intermediate buffers, since the GEMM between tensor $[N, B, C]$ and weight $[\hat{C}, C]$ generates an intermediate buffer $[N, B, \hat{C}]$ regardless of C . Activation checkpoint (**AC.**) is also a commonly used strategy in large model training, as it can significantly reduce the GPU memory pressure for models with many layers. Activation checkpoint with offloading (**OC.**) is a technique introduced in DeepSpeed, which allows the checkpointed activation to be moved to host memory. Both **AC.** and **OC.** play critical roles in enlarging the sequence length, i.e., from 32K to 128K to 512K. For Ulysses, it can seamlessly work with the ZeRO family, which reduces a decent amount of memory footprint, i.e., from 58.9G to 52.3G. However, ZeRO doesn’t mitigate the memory requirement for long-context LLM training as it reduces only memory usage related to the model parameters. Finally, our proposed FPDT, together with activation checkpointing, activation of offloading, and ZeRO-3, remarkably increases the maximum sequence length by 8x, from 512K to 4M, on an 8B Llama 3 with 8 GPUs, while achieving extreme hardware efficiency.

5.6 Convergence evaluation

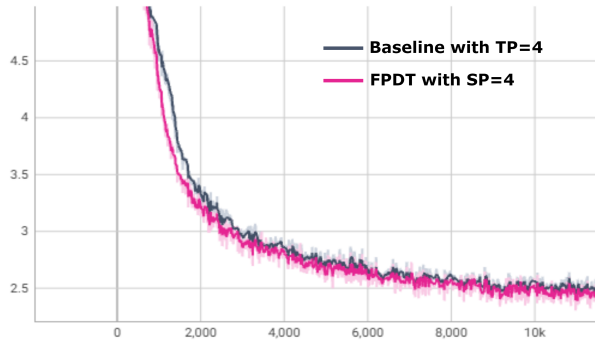


Figure 14. Loss curve in pretraining GPT models with 4 GPUs.

Figure 14 shows the convergence of the baseline GPT model that leverages tensor parallel on 4 GPUs, with a batch size of 256 and ZeRO-1 enabled, and our FPDT w/ and w/o offloading. Our proposed FPDT is a pure system optimization technique that enables the training of ultra-long sequence Transformer model, thus there is no (negative) on the quality of trained models.

6 FUTURE WORK

This paper focuses on alleviating the memory constraints that are brought by the activations and intermediate buffers in long-sequence LLM training. We conduct experiments with the ZeRO-3 technique. However, we noticed that PyTorch here can also incur a high memory spike when it reduces the gradients across all GPUs. In certain cases, this memory spike can be more significant than the activation’s memory spikes, which becomes a bottleneck in keeping increasing sequence length. We will investigate this and welcome researchers in this field to advance long-sequence LLM training together.

7 CONCLUSION

In this paper, we present the Fully Pipelined Distributed Transformer (FPDT), for efficiently training long-sequence LLMs within resource-constrained environment. Our proposed method leverages advanced sequence parallelism and ZeRO-3, largely reducing the GPU resource required for million-level sequence training. With our elaborately designed overlapping scheme, training 2.7B to 70B LLMs on up to 4M token sequence with FPDT reaches over 55% MFU. Our method can also be applied to LLMs with Transformer-like blocks with little re-configuration. We believe our work can benefit the large community in exploring LLMs’ capability in long context scenarios.

REFERENCES

- Ainslie, J., Ontanon, S., Alberti, C., Cvicek, V., Fisher, Z., Pham, P., Ravula, A., Sanghai, S., Wang, Q., and Yang, L. Etc: Encoding long and structured inputs in transformers. *arXiv preprint arXiv:2004.08483*, 2020.
- Beltagy, I., Peters, M. E., and Cohan, A. Longformer: The long-document transformer. *arXiv preprint arXiv:2004.05150*, 2020.
- Child, R., Gray, S., Radford, A., and Sutskever, I. Generating long sequences with sparse transformers. *arXiv preprint arXiv:1904.10509*, 2019.
- Dao, T. Flashattention-2: Faster attention with better parallelism and work partitioning. *arXiv preprint arXiv:2307.08691*, 2023.
- Dao, T., Fu, D., Ermon, S., Rudra, A., and Ré, C. Flashattention: Fast and memory-efficient exact attention with io-awareness. *Advances in Neural Information Processing Systems*, 35:16344–16359, 2022.
- Eisfeldt, A. L., Schubert, G., and Zhang, M. B. Generative ai and firm values. Technical report, National Bureau of Economic Research, 2023.
- Gao, S., Alawad, M., Young, M. T., Gounley, J., Schaeferkoetter, N., Yoon, H. J., Wu, X.-C., Durbin, E. B., Doherty, J., Stroup, A., et al. Limitations of transformers on clinical text classification. *IEEE journal of biomedical and health informatics*, 25(9):3596–3607, 2021.
- Jacobs, S. A., Tanaka, M., Zhang, C., Zhang, M., Song, L., Rajbhandari, S., and He, Y. Deepspeed ulysses: System optimizations for enabling training of extreme long sequence transformer models. *arXiv preprint arXiv:2309.14509*, 2023.
- Katharopoulos, A., Vyas, A., Pappas, N., and Fleuret, F. Transformers are rnns: Fast autoregressive transformers with linear attention. In *International conference on machine learning*, pp. 5156–5165. PMLR, 2020.
- Kim, A., Muhn, M., and Nikolaev, V. From transcripts to insights: Uncovering corporate risks using generative ai. *arXiv preprint arXiv:2310.17721*, 2023.
- Kim, A., Muhn, M., and Nikolaev, V. V. Bloated disclosures: can chatgpt help investors process information? *Chicago Booth Research Paper*, (23-07):2023–59, 2024.
- Kitaev, N., Kaiser, Ł., and Levskaya, A. Reformer: The efficient transformer. *arXiv preprint arXiv:2001.04451*, 2020.
- Korthikanti, V. A., Casper, J., Lym, S., McAfee, L., Andersch, M., Shoeybi, M., and Catanzaro, B. Reducing activation recomputation in large transformer models. *Proceedings of Machine Learning and Systems*, 5:341–353, 2023.
- Li, Y., Wehbe, R. M., Ahmad, F. S., Wang, H., and Luo, Y. Clinical-longformer and clinical-bigbird: Transformers for long clinical sequences. *arXiv preprint arXiv:2201.11838*, 2022.
- Li, Y., Wang, S., Ding, H., and Chen, H. Large language models in finance: A survey. In *Proceedings of the fourth ACM international conference on AI in finance*, pp. 374–382, 2023.
- Liu, H. and Abbeel, P. Blockwise parallel transformers for large context models. *Advances in Neural Information Processing Systems*, 36, 2024.
- Liu, H., Zaharia, M., and Abbeel, P. Ring attention with blockwise transformers for near-infinite context. *arXiv preprint arXiv:2310.01889*, 2023.
- Liu, Z., Lin, Y., Cao, Y., Hu, H., Wei, Y., Zhang, Z., Lin, S., and Guo, B. Swin transformer: Hierarchical vision transformer using shifted windows. In *Proceedings of the IEEE/CVF international conference on computer vision*, pp. 10012–10022, 2021.
- Lu, J., Yao, J., Zhang, J., Zhu, X., Xu, H., Gao, W., Xu, C., Xiang, T., and Zhang, L. Soft: Softmax-free transformer with linear complexity. *Advances in Neural Information Processing Systems*, 34:21297–21309, 2021.
- Luo, C., Zhao, J., Chen, Z., Chen, B., and Anandkumar, A. Mini-sequence transformer: Optimizing intermediate memory for long sequences training. *arXiv preprint arXiv:2407.15892*, 2024.
- MosaicML. Introducing mpt-7b: A new standard for open-source, commercially usable llms. <https://www.mosaicml.com/blog/mpt-7b>, 2023. Accessed: 2024-08-29.
- Munkhdalai, T., Faruqui, M., and Gopal, S. Leave no context behind: Efficient infinite context transformers with infini-attention. *arXiv preprint arXiv:2404.07143*, 2024.
- Nguyen, T., Brandstetter, J., Kapoor, A., Gupta, J. K., and Grover, A. Climax: A foundation model for weather and climate. *arXiv preprint arXiv:2301.10343*, 2023.
- Peng, B., Quesnelle, J., Fan, H., and Shippole, E. Yarn: Efficient context window extension of large language models. *arXiv preprint arXiv:2309.00071*, 2023.

- Rajbhandari, S., Rasley, J., Ruwase, O., and He, Y. Zero: Memory optimizations toward training trillion parameter models. In *SC20: International Conference for High Performance Computing, Networking, Storage and Analysis*, pp. 1–16. IEEE, 2020.
- Su, J., Ahmed, M., Lu, Y., Pan, S., Bo, W., and Liu, Y. Roformer: Enhanced transformer with rotary position embedding. *Neurocomputing*, 568:127063, 2024.
- Touvron, H., Martin, L., Stone, K., Albert, P., Almahairi, A., Babaei, Y., Bashlykov, N., Batra, S., Bhargava, P., Bhosale, S., et al. Llama 2: Open foundation and fine-tuned chat models. *arXiv preprint arXiv:2307.09288*, 2023.
- Vaswani, A. Attention is all you need. *Advances in Neural Information Processing Systems*, 2017.
- Wang, S., Li, B. Z., Khabsa, M., Fang, H., and Ma, H. Linformer: Self-attention with linear complexity. *arXiv preprint arXiv:2006.04768*, 2020.
- Xiong, W., Liu, J., Molybog, I., Zhang, H., Bhargava, P., Hou, R., Martin, L., Rungta, R., Sankararaman, K. A., Oguz, B., et al. Effective long-context scaling of foundation models. *arXiv preprint arXiv:2309.16039*, 2023.
- Xiong, Y., Zeng, Z., Chakraborty, R., Tan, M., Fung, G., Li, Y., and Singh, V. Nyströmformer: A nyström-based algorithm for approximating self-attention. In *Proceedings of the AAAI Conference on Artificial Intelligence*, volume 35, pp. 14138–14148, 2021.
- Yang, H., Liu, X.-Y., and Wang, C. D. Fingpt: Open-source financial large language models. *arXiv preprint arXiv:2306.06031*, 2023.
- Zaheer, M., Guruganesh, G., Dubey, K. A., Ainslie, J., Alberti, C., Ontanon, S., Pham, P., Ravula, A., Wang, Q., Yang, L., et al. Big bird: Transformers for longer sequences. *Advances in neural information processing systems*, 33:17283–17297, 2020.
- Zhao, P., Zhang, H., Fu, F., Nie, X., Liu, Q., Yang, F., Peng, Y., Jiao, D., Li, S., Xue, J., et al. Efficiently training 7b llm with 1 million sequence length on 8 gpus. *arXiv preprint arXiv:2407.12117*, 2024.
- Zhao, Y., Gu, A., Varma, R., Luo, L., Huang, C.-C., Xu, M., Wright, L., Shojanazeri, H., Ott, M., Shleifer, S., et al. Pytorch fsdp: experiences on scaling fully sharded data parallel. *arXiv preprint arXiv:2304.11277*, 2023.
- Zvyagin, M., Brace, A., Hippe, K., Deng, Y., Zhang, B., Bohorquez, C. O., Clyde, A., Kale, B., Perez-Rivera, D., Ma, H., et al. Genslms: Genome-scale language models reveal sars-cov-2 evolutionary dynamics. *The International Journal of High Performance Computing Applications*, 37(6):683–705, 2023.